High-speed and High-power-density Quasi-Coreless PMSM for Vehicle Propulsion

Takashi Kosaka, Teruchika Ishihara and Ayaka Sakuma

Nagoya Institute of Technology, Gokiso, Showa, Nagoya, Japan

E-mail: kosaka.takashi@nitech.ac.jp

ABSTRACT: This paper deals with a high-speed and high-power density quasi-coreless permanent magnet synchronous motor for vehicle traction drives. Stator body is composed of carbon fiber reinforced plastic, a small amount of soft magnetic composite core and aluminum windings. Rotor body consists of polar anisotropic magnets and carbon fiber reinforced plastic as a retaining sleeve. FEA-based design study on a 150kW quasi-coreless permanent magnet synchronous motor rotating at 50,000r/min as the maximum speed with high-power density more than 10kW/kg is reported. In particular, this paper focuses on the mechanical design considering assembly process of the rotor. To verify the rotor mechanical design, high-speed spin test results using a prototype of rotor assembly built are demonstrated.

KEY WORDS: quasi-coreless permanent magnet synchronous motor, high-speed motor, high-power density, electric vehicle drive

1. INTRODUCTION

Recently, a reduction of CO_2 emissions from transportation sector among industrial sectors is indispensable task, which accounts for 23% of the total CO_2 emissions. This has accelerated decarbonization by an electrification of ships, aircrafts and automobiles so that electric motors with higher power density are in demand(1). One well-known approach for elevating specific-power density (kW/kg) is to design the electric motor rotating very high-speed while maintaining torque as much as possible, considering the reduction gear ratio(2)~(3). However, there are a lot of concerns, for examples, as an increase in iron losses due to higher frequency components of magnetic field in the electric motor at the high-speed region and the mechanical design difficulty in high-speed rotor.

To elevate the specific-power density further, the authors have proposed a three-phase quasi-coreless permanent magnet synchronous motor (hereinafter referred to as quasi-coreless SPMSM) with high speed rotation aimed at further weight reduction and iron loss reduction(4). The rotor consists of polar anisotropic magnets and carbon fiber reinforced plastic as a retaining sleeve. The stator is composed of carbon fiber reinforced plastic (CFRP) as the structure support member, a small amount of soft magnetic composites core (SMC core)(5), and aluminum windings(6). CFRP has a specific gravity of approximately 1/4 that of iron at 1.6g/cm³, and its yield strength is approximately 4 times of that of iron in the fiber direction more than 1500MPa. To prevent torque reduction due to the decrease in gap flux density caused by coreless design, the proposed quasi-coreless SPMSM employs a minimal SMC core in the CFRP structure support member of the stator. The SMC core, being an iron core made by compressing iron powder coated with an insulating layer, can suppress iron losses, in particular, eddy current losses due to high frequency components of internal magnetic fields at high-speed operation. Compared with the conventional stator core made of electromagnetic steel sheets, therefore, the use of small amount of SMC embedded in the CFRP structure support member could contribute to weight reduction while suppressing the increase in iron losses for the high-speed electric motors.

In addition to advantages in terms of economy and sustainability, employing aluminum winding is another approach to increase the specific-power density. The aluminum conductor whose specific gravity is 2.7g/cm³ approximately one third of that of the copper's one 8.96g/cm³ can reduce motor weight further. It also reduces eddy current losses known as winding AC losses caused by the direct linkage of high-frequency flux with the windings thanks to the high resistivity of 2.65×10^{-8} Ω·m at 20C°, which is approximately 1.6times higher than that of the copper. Needless to say, the design to suppress DC copper loss becomes a challenge in this case, but it is effective further reduction of AC losses(6).

In Ref. (4), design feasibility study on a quasi-coreless SPMSM for a traction motor drive targeting the maximum rotational speed of 50,000r/min, the maximum output of 150kW, and the maximum-power density more than 10kW/kg has been reported. Following this feasibilty study, this paper presents secondary

design investigation of high-speed rotor with 80mm diameter investigation taking its fabrication process into account. Moreover, a rotor with larger diameter of 140mm for spin test to validate the secondary high-speed rotor design concept while keeping same design concept of the rotor with 80mm diameter is designed and built. The spin test result validates the high-speed rotor design concept rotating at 50,000r/min as the target maximum speed.

2. PRIMARY DESIGN OF QUASI-CORELESS SPMSM(4)

2.1. Summary of primary design result

Fig. 1 shows a cross-sectional view of the quasi-coreless three-phase SPMSM proposed and designed primary using two-dimensional and three-dimensional finite element analysis (JMAG-Designer Ver. 23.0.0.1, hereinafter referred to as 2D- and 3D-FEA)(4).

The rotor is composed of a CFRP sleeve with 2mm thickness on the outer circumference of the permanent magnets (PMs) to prevent scattering the PMs due to centrifugal force during high-speed rotation at 50,000r/min. The rotor inner circumference also employs CFRP for weight reduction. As CFRP has a relative permeability equivalent to air, a polar anisotropic magnet is used without making the rotor inner circumference a magnetic circuit, similar to a Halbach array magnet, to enhance air gap flux density.

The stator body is made of the aforementioned CFRP, SMC core and aluminum winding. An increase in a number of short-pitch coils can increase the heat dissipation surface area per loss, improve torque density with more poles, and reduce copper losses with high winding factors and short coil end lengths. On the other hand, it is necessary to suppress the increase in inverter switching frequency for high-speed machine. Considering this balance, 8-pole, commonly adopted in current automobile traction motors, was selected. For 8-pole machine, a concentrated short-pitch winding with a high winding factor would ideally be a 9-slot configuration, but this causes unbalanced magnetic pull on the rotor. Therefore, distributed winding is adopted, and a 48-slot distributed winding with q=2 (q: slots per pole per phase) is used to suppress harmonic components of the spatial magnetomotive force and reduce winding AC losses as well as eddy current loss in the PMs.

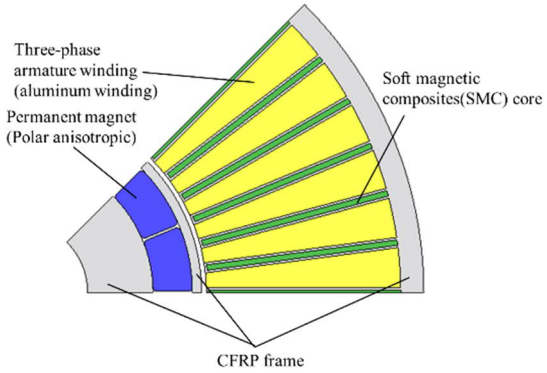

Fig. 1. Sectional view of quasi-coreless PMSM (1/8 cut model).

For a SPMSM with 48slot/8pole combination, the quasi-coreless structure employing a little SMC core forming the stator tooth with CFRP has been introduced. Even though a very high maximum current density of $20A_{rms}/mm^2$ has been set for the armature winding under water cooling, it has been difficult to achieve the target performance by a complete coreless structure without a use of SMC core. Fig. 2 presents a comparison between the flux density contour diagrams computed by 2D-FEA under the same maximum ampere-turns for the coreless SPMSM without employing SMC core and the quasi-coreless SPMSM employing the SMC core with 1.2mm thickness. As apparent from the figure, before inserting the SMC cores, little flux passes through to the center of the winding in the radial direction. In contrast, after the SMC cores are inserted, a large amount of fluxes passes through to the center. As a result, the maximum torque achieved by the designed primary quasi-coreless SPMSM reaches 2.57 times of that of the coreless SPMSM. Whereas, the total motor weight after inserting the SMC core is only 29% higher than that of the coreless

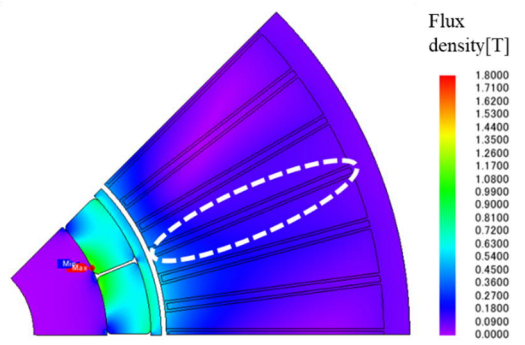

(a) without employing SMC core

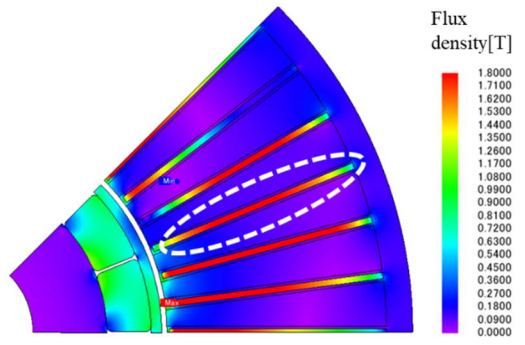

(b) with SMC core

Fig. 2. Comparison of flux density contour diagrams under the same maximum ampere-turns condition for the coreless and the quasi-coreless SPMSM.

SPMSM before inserting the SMC core. Consequently, the specific-torque density of the quasi-coreless SPMSM becomes double of that of the coreless SPMSM so that the design concept of the quasi-coreless structure employing a little SMC core is effective from a viewpoint of higher specific-torque and -power densities.

Table 1 appears the specifications and the drive performances evaluated by 2D- and 3D-FEA of the designed primary quasi-coreless SPMSM. The total motor weight excludes the weights of coil ends and bearings. Under the inverter DC bus voltage of 800V, the base speed of the designed quasi-coreless PMSM reaches 13,300 r/min, meeting the target base speed of 12,500 r/min. The maximum torque almost meets the design target requirement for 114.6N·m. Beyond the base speed, the constant power speed range over 150 kW can be achieved by flux weakening control. As a result, the specific-power density of the designed motor reaches 17.8 kW/kg that is 1.78 times of the target value of 10 kW/kg. The power factor at the operating point, 13,300r/min-114.5N·m-159.6kW, is as low as 0.49. This results in the increase in the maximum inverter current as large as 319 Arms. The DC copper loss in the aluminum windings at the same operating point is 11.2kW at 20 C° and the iron loss in the SMC core is 0.82kW. The motor efficiency calculated considering all losses mentioned above is 93.0%. Note that the AC loss of the aluminum armature windings is not considered to calculate the motor efficiency. The AC loss consideration will be done later after determining how to build the stator assembly.

Table 1 Specifications and drive performances of the designed primary quasi-coreless SPMSM.

Poles/Slots	8/48
Rotor outer diameter [mm]	80
Rotor CFRP sleeve thickness [mm]	2
Stator outer diameter [mm]	176
Stator/rotor axial length [mm]	144
Mechanical airgap [mm]	1
No. of turns/slot	7
Total motor weight excluding coil-end and bearing weights [kg]	9.0
Inverter DC bus voltage[V]	800
Inverter maximum current I_{max} [A_{rms}]	319
Base speed N_{base} [r/min]	13,300
Maximum torque [N·m]	114.5
Maximum power@114.5N·m-13,300r/min [kW]	159.6
Torque density [Nm/kg]	12.8
Power density [kW/kg]	17.8
DC copper loss of Al armature windings [kW]	11.2
Iron loss in SMC core [kW]	0.82
Eddy current loss in PMs @114.5N·m-13,300r/min[W]	20.7
Motor efficiency @ 114.5N·m-13,300r/min[W]	93.0

2.2. Primary structural design of stator assembly

Lorentz force arisen in the windings and Maxwell's stress occurred in the SMC core are analyzed because they are particularly concerning among internal stresses, resulting in a risk of the stator assembly broken. The aluminum windings are treated as a composite material of aluminum and varnish to evaluate the Lorentz force on the windings and the Maxwell's stress on the SMC core because there is a possibility that stress may be underestimated if the winding section is treated as a solid block of aluminum supporting the CFRP teeth. The equivalent Young's modulus and equivalent Poisson's ratio are introduced and used to assign equivalent material properties[4].

At first, analysis (a) considering only Lorentz force on the windings and analysis (b) considering only Maxwell's stress on the SMC core are conducted under the condition of compaction coefficient C=0.2. The values of the maximum von Mises stress are shown in Table 2. The analysis results indicate that the Maxwell's stress is more dominant than the Lorentz force on the windings. Next, analysis considering only Maxwell's stress on the SMC core is conducted with varying values of the compaction coefficient C. The values of the maximum von Mises stress are shown in Table 3. The contour plot of stress concentration in the teeth for the worst-case scenario of the compaction coefficient C=0 is shown in Fig. 3. The maximum von Mises stress for the worst-case scenario of the compaction coefficient C=0 is approximately 90MPa, indicating that there is sufficient margin against the bending strength of 900MPa for CFRP. It is expected that stress concentration can be further alleviated by removing sharp angles and applying curved surface treatment. Based on these results, it is concluded that the primary structural design of

Table 2 Analyzed maximum Von-Mises stresses.

	Max. Von Mises stress [MPa]
(a) Winding Lorentz force	0.24
(b) Maxwell's stresses on SMC	31.24

Table 3 Analyzed maximum Von-Mises stresses (C=0~0.6).

	Max. Von-Mises stress [MPa]
C=0	89.57
C=0.2	31.24
C=0.4	23.81
C=0.6	19.99

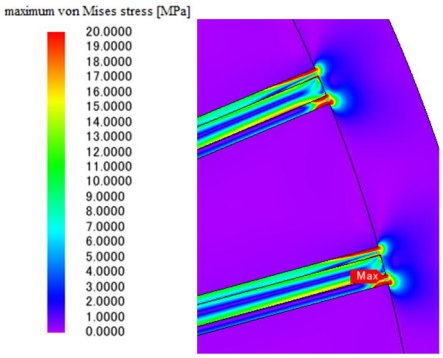

Fig. 3. Contour plot of Von-Mises Stress (C=0).

the stator assembly has no risk of broken due to both the Lorentz force on the windings and the Max-well's stress on the SMC core.

2.3. Primary structural design of rotor assembly

In this primary design, a CFRP sleeve with a fracture strength of 1500 MPa in the fiber direction is used to prevent centrifugal force dispersion of PMs at 50,000r/min as the maximum speed. From a viewpoint of weight reduction, CFRP is also used on the inner circumference of the rotor, forming the rotor body. From the perspective of torque density, a larger outer diameter of rotor magnet is better, but it increases the centrifugal force on rotor magnets. While a thicker CFRP sleeve can ensure mechanical strength for a larger diameter of rotor PMs, it increases the equivalent air gap, leading to a decrease in gap flux density. Considering these trade-offs, rotor stress analysis has been conducted at the maximum speed of 50,000 r/min to determine the rotor outer diameter. Prior to determining the rotor outer diameter, considering manufacturing dimensional constraints, the magnet thickness was set to 8.5 mm. The thickness of the CFRP sleeve has been set to 2 mm and the mechanical airgap length has been set to 1 mm as shown in Table 1.

The stress analysis solver in JMAG-Designer Ver. 23.0.01 is used for rotor stress analysis. Contact conditions with a friction coefficient of 0.3 are set between the inner circumference CFRP and the PMS and between the PMs and the CFRP sleeve. Binding conditions in the circumferential direction are set to each border surface of 1/16 rotor model shown in Fig. 4. Under these conditions, the variation in the maximum von Mises stress on the CFRP sleeve with respect to rotor radius variation is plotted in Fig. 5. Considering a safety factor of 1.3 against CFRP fracture strength of 1500 MPa, the maximum von Mises stress is 1154 MPa. The rotor radius that satisfies this value is determined to be 40 mm.

3. SECONDARY STRUCTURAL ROTOR DESIGN

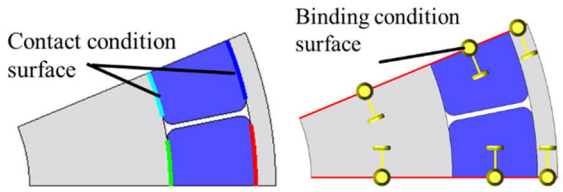

(a) contact condition (b) binding condition

Fig. 4. Concact and binding conditions set in stress analaysis.

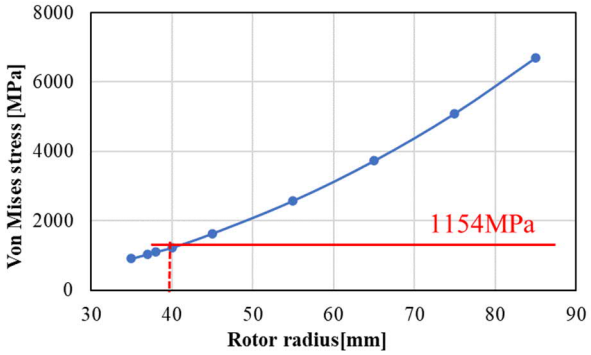

Fig. 5. Analysis result of the maximum von Mises stress of CFRP sleeve with respect to rotor radius change.

Following the primary rotor design mentioned in Subsection 2.3, the secondary structural design of the rotor assembly is examined considering fabrication process for prototyping. Fig. 6 illustrates a sectional view of the designed secondary rotor. Considering fabrication process of the high-speed rotor, the rotor structure is changed from the designed primary rotor to the designed secondary one as follows. At first, the inner circumference CFRP is replaced with a duralumin block to provide keyways structure for fixing the rotor body on shaft. The duralumin has relatively high tensile strength of 425Mpa. Since there is no clear yield point for the duralumin, instead 0.2% yield strength is used for stress analysis, which is 275MPa. Although the specific gravity is 2.79g/cm^3 heavier than that of CFRP (1.6g/cm^3), it still allows to keep the target specific-power density more than 10kW/kg. On the other hand, as the duralumin has conductivity, eddy current loss on the surface becomes concern. Eddy current analysis is conducted to check the eddy current loss on the duralumin block. According to the eddy current analysis, it is found that there is no flux density variation at any point on the surface of the duralumin block operating point at 13,300r/min- 114.5Nm- 159.6kW. Therefore, no eddy current loss occurs on the surface of the duralumin block. The PMs are attached on the surface of the duralumin block without adhesives. After fixing the PMs, pre-impregnated is wound on the PM's surface and making CFRP after heat treatment in autoclave.

Corresponding to the fabrication process mentioned above, stress analysis of the designed secondary rotor structure shown in

Fig. 6 is conducted. Contact conditions with no friction are set between the inner circumference duralumin block and the PMs and between the PMs and the CFRP sleeve as shown in Fig. 7(a). Binding conditions in the circumferential direction are set at the center line of each PM and at the structurally symmetric axes as shown in Fig. 7(b). Fig. 8 shows the stress analysis result of the secondary rotor at the maximum speed of 50,000r/min under these contact and binding conditions. It can be seen in the figure that the maximum von Mises stress on the CFRP sleeve reaches 1214MPa, which is slightly higher than the allowable maximum von Mises stress of 1154MPa under the consideration of the safety factor of 1.3 against CFRP fracture strength of 1500MPa. The maximum von Mises stress on the duralumin block is 262.4MPa, which is slightly smaller than 275MPa as 0.2% yield strength of the duralumin. The maximum von Mises stress on the PMs is less than 100MPa. This stress is not only allowable maximum stress of the PMs, but also a compressed stress. Therefore, it is reasonable to suppose that the PMs has no risk of broken at the maximum rotor speed, 50,000 r/min.

4. SPIN TEST USING PROTOTYPE ROTOR

4.1. Prototype of rotor for high-speed spin test

Based on the design concept same with the secondary rotor, a prototype of rotor is designed and built for a high-speed spin test.

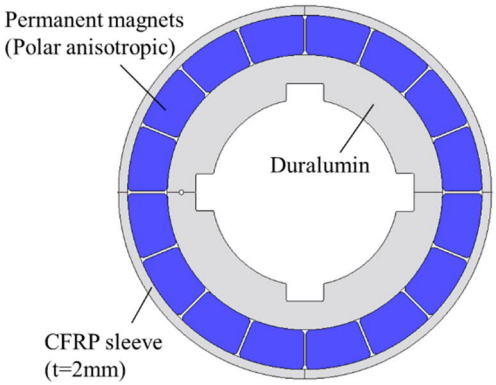

Fig. 6. Sectional view of the secondary rotor designed.

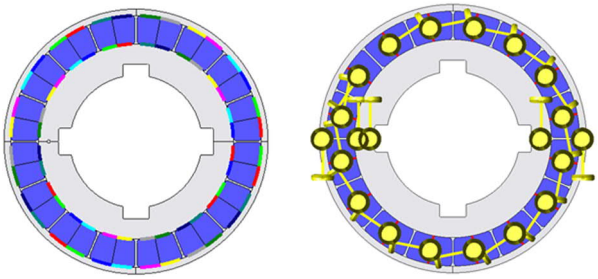

(a) contact condition (b) binding condition

Fig. 7. Concact and binding conditions set in stress analaysis for the secondary rotor designed.

The high-speed spin test is conducted at Maruwa Electronic Inc.[7]. Considering the high-speed spin tester specifications, a prototype of rotor is designed so as to be broken near around at 30,000r/min. The original secondary design rotor has been designed with a diameter of 80 mm, whereas the prototype rotor for the high-speed spin test has been designed with a diameter of 140 mm. Fig. 9 depicts a sectional view of the prototype rotor. Similarly, stress analysis of the designed prototype rotor structure shown in Fig. 9 is conducted. Fig. 10 is the stress analysis result of the prototype rotor at the maximum speed of 30,000r/min under the contact and binding conditions same with those used in the stress analysis of the secondary rotor. From the figure, it is found that the maximum von Mises stress on the CFRP sleeve reaches 1529MPa, which is higher than the CFRP fracture strength of 1500 MPa. This means the prototype rotor design has no consideration of the safety factor of CFRP sleeve rotating at 30,000r/min. The maximum von Mises stress on the duralumin block is 290MPa, which is slightly higher than 275MPa as 0.2% yield strength of the duralumin. The maximum von Mises stress on the PMs is 75.2Mpa. This stress is not only allowable maximum stress of the PMs, but also a compressed stress. Fig. 11 shows a photograph of the prototype rotor.

4.2. High-speed spin test result

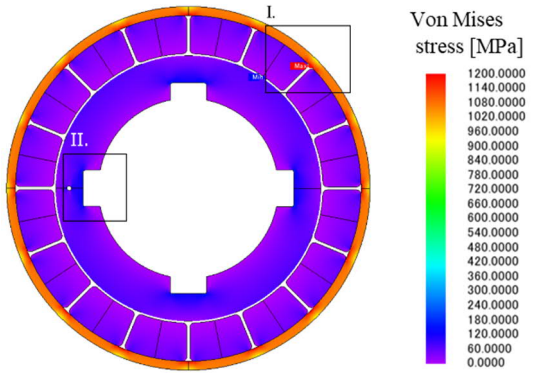

(a) whole rotor view

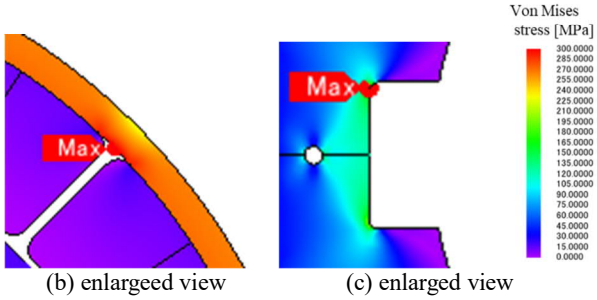

(b) enlargeed view near around I (c) enlarged view near around II

Fig. 8 Contour plot of Von-Mises Stress analyzed for the secondary rotor designed at 50,000r/min.

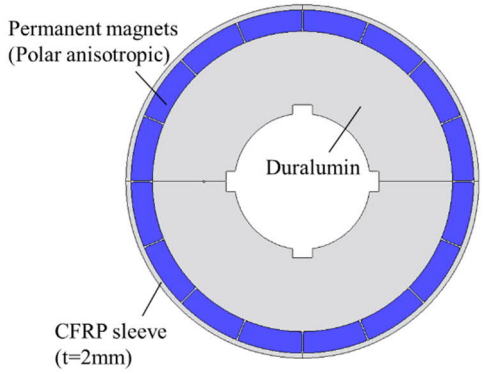

Fig. 9. Sectional view of the prototype rotor for spin test.

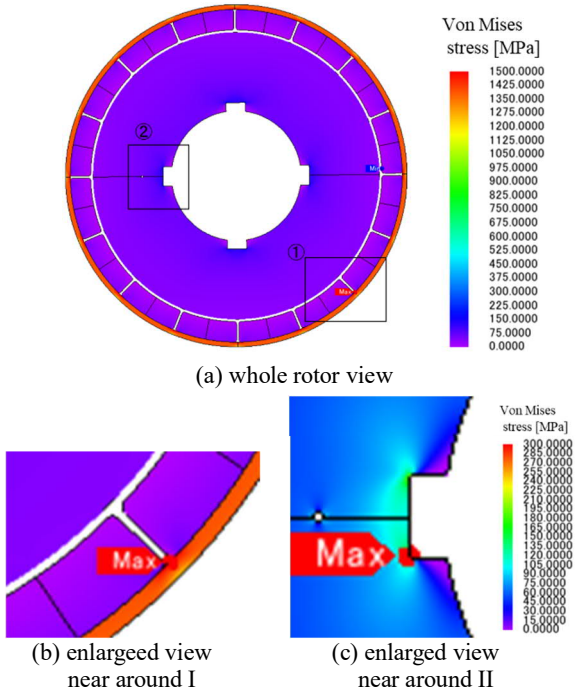

(a) whole rotor view

(b) enlargeed view near around I

(c) enlarged view near around II

Fig. 10 Contour plot of Von-Mises Stress analyzed for the prototype rotor designed at 30,000r/min.

The high-speed spin test using the prototype rotor shown in Fig. 11 has been executed while varying the rotor test speed from 3,000 to 30,000r/min. Up to 25,000r/min, no change of the outer diameter of the prototype rotor has been observed. However, the rotor outer diameter expansion with 40μm has been confirmed after the spin test rotating at 26,000r/min. Then, it has been confirmed that the wound end of the CFRP sleeve on the rotor surface has peeled off after the test rotating at 27,000r/min. Finally, the spin test at 28,000r/min has been done as shown in Fig. 12, checking whether the further broken happens or not, but no change of the rotor structure has observed. From these results, it seems reasonable to suppose that the secondary rotor design concept considering the safety factor of 1.3 for the CFRP fracture strength of 1500 MPa is valid for the high-speed rotor design at the maximum speed of 50,000r/min.

Fig. 11. Photgraph of the prototype rotor.

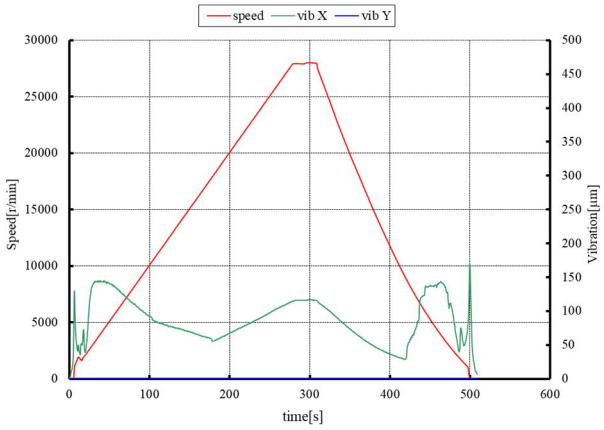

Fig. 12. Spin test result at 28,000r/min.

5. CONCLUSIONS

This paper presented the secondary design of the quasi-coreless SPMSM with a target of 50,000 r/min as the maximum speed, 150 kW as the maximum output and over 10 kW/kg of power density, using CFRP for the main frame, polar anisotropic magnets, and aluminum windings. In particular, the secondary rotor design was emphasized on and the secondary rotor design concept was validated by the high-speed spin test using a prototype rotor.

ACKNOWLEDGMENT

This paper is based on results obtained from a subcontract from Transmission Research Association for Mobility Innovation (TRAMI) as part of the New Energy and Industrial Technology Development Organization (NEDO) Feasibility Study Program on New Energy and Environmental Technology / Resource saving of electric drive system for automobiles by ultra-high rotation of e-motor. (JPNP14004).

REFERENCES

(1) NEDO, “Green Innovation Fund Projects / Automobiles and Battery Industries”,

https://green-innovation.nedo.go.jp/project/next-generation-storage-batteries-motors/

(2) D. Gerada, A. Mebarki, N. Brown and C. Gerada, “High-speed electrical machines: technologies trends and developments”, IEEE Trans. on IE., Vol. 61, No. 6, pp. 2946-2959 (2014)

(3) M. Enokizono, D. Wakabayashi, N. Soda, Y. Tsuchida, S. Ueno and M. Oka, “High Power Density and High Efficiency of High-speed Motor”, 2020 International Conference on Electrical Machines (ICEM), pp.170-176 (2020)

(4) T. Kosaka, T. Ishihara and A. Sakuma, “Design Study on High Power Density Quasi-Coreless PMSM for Vehicle Traction Drive Rotating at 50,000r/min as the Maximum Speed”, Proc. of 2024 27th International Conference on Electric Machines and Systems (ICEMS2024), pp.2675-2680 (2024).

(5) T. Saito, Y. Enokizono, D. Higashi, T. Ishimine, T. Ueno, Y. Nakamura and R. Okuno, “Enhanced Functionality of Soft Magnetic Composites for High-Performance Axial Gap Motors”, SEI Technical Review, No. 198, pp. 41-46 (2021)

(6) Yuto Yamada, Jun Ebinuma and Hiroya Sugimoto, “High Slot Fill Aluminum Distributed Winding for High-Speed and High Power Density Electric Machines”, Proc. of 2024 27th International Conference on Electric Machines and Systems (ICEMS2024), pp.1890-1896 (2024).

(7) Maruwa Electronic Inc., https://www.maruwa-denki.co.jp/en.html